Alternating Gradient Synchrotron Department
Relativistic Heavy Ion Collider Project
BROOKHAVEN NATIONAL LABORATORY
Upton, New York 11973

Spin Note

AGS/RHIC/SN No. 048

Analytical Field Calculation of the Direct Wind Helical Dipole

T. Tominaka

December 18, 1996

For Internal Distribution Only

Analytical Field Calculation of the Direct Wind Helical Dipole

T. Tominaka (RIKEN, Japan)

1. Introduction

The magnetic field of a prototype of the direct wind helical dipole fabricated at AML, Inc. under contract with BNL, is calculated analytically and numerically in this paper. The analytical calculation is compared with the numerical calculation by the Biot and Savart's Law in the case without iron yoke. The purpose of this paper is to obtain the contents of multipoles expected for the direct wind helical dipole.

2. Shape of a Direct Wind Helical Dipole Magnet

A schematic views of some portions of this superconducting helical dipole are shown in Fig.1. The cross sections at z=0 and z=0.4 m of this superconducting helical dipole are shown in Figs.2 and 3, respectively. All 1866 black dots shown in Figs.2 and 3 correspond to superconducting strands used as conductors. These figures are derived from the data of 202524 points about the helical dipole coil with 11 layers. Then, the central or average angle of both coil blocks can be obtained as the average of every conductor's angle in each block. In addition, the z dependence of the central angle of both coil blocks is obtained, as shown in Figs.4 and 5. By fitting, the z [m] dependence of the central angle, $\theta_r(z)$, $\theta_l(z)$ [rad] of the right and left coil block at z=0 are as follows,

$$\begin{cases} \theta_r(z) = 0.00376105 + 2.51957\, z + 8.03707\ 10^{-6}\, z^2 - 0.0000319832\, z^3 \\ \theta_l(z) = 3.13783 + 2.51957\, z - 8.03707\ 10^{-6}\, z^2 - 0.0000319832\, z^3 \end{cases} \qquad (1)$$

From this equation, it results that $k=2\pi/L=2.52$ rad/m, and $\theta_r(z=0) > 0$ and $\theta_l(z=0) < \pi$, where L is the pitch length. Then, it is realized that both coil blocks are wholly little bit closer to the upper pole than the lower pole at z=0. As a result, it is expected that this prototype of the direct wind helical dipole has the skew multipoles.

3. Magnetic Field of a Direct Wind Helical Dipole Magnet

For the case of current, I = 420 A, without iron yoke, the magnetic field of this prototype of the direct wind helical dipole magnet is calculated numerically with the Biot and Savart's Law from the data of 202524 points, as shown in Figs.6 and 7. The conventional normal multipole coefficients can also be derived by fitting from the y component of magnetic field, B_y, on the x-axis as shown in Fig.6. The resultant expression is as follows,

$$B_y(r=x,\theta=0,z=0) = 2.366 \left\{ 1 - 0.0121 \left(\frac{x}{r_0}\right)^2 - 0.0117 \left(\frac{x}{r_0}\right)^4 + 0.00356 \left(\frac{x}{r_0}\right)^6 - 7.9\ 10^{-4} \left(\frac{x}{r_0}\right)^8 + 4.3\ 10^{-4} \left(\frac{x}{r_0}\right)^{10} \right\} \qquad (2)$$

In addition, the conventional normal and skew multipole coefficients for the reference radius r_0 = 30 mm, from the y-directional magnetic field B_y on the circle of radius r= 30 mm can be derived with the Fourier analysis, as shown Table 1. For example, the conventional sextupole coefficients b_3 = - 0.0121 derived from the field distribution of B_y on x-axis is different from b_3 = - 0.0136 derived from the field distribution on the circle due to the helical structure.

The normal and skew contents of helical multipole with the reference radius r_0 = 30 mm, can be analytically calculated from the distribution of the radial magnetic field B_r, the azimuthal magnetic field B_θ, and the z-directional magnetic field B_z on the circle of radius r= 30 mm calculated numerically with the Biot and Savart's Law, as shown in Table 2.

Furthermore, in the case without iron yoke, the magnetic field of a direct wind helical dipole magnet can be calculated analytically with the assumption of the infinite length with the coil twist of k=2.52 rad/m. For the comparison, the analytically calculated contents of helical multipole expected for this helical dipole together with the 2-dimensional multipole coefficients of the 2-dimensional structure for the reference radius r_0 = 30 mm, are shown in

Tables 3 and 4, respectively. From comparison between Tables 2 and Table 3, it is realized that the analytical results are almost consistent with those obtained numerically with the Biot and Savart's Law for this prototype of the direct wind helical dipole. The twist (or k) dependence of the reference field $B_{ref}(k)$, the helical skew quadrupole coefficient. $a_2(k)$, and the helical normal sextupole coefficient, $b_3(k)$, are shown in Figs.8, 9 and 10, respectively.

In the case with iron yoke of the inner diameter of 127.6 mm, similarly, the analytically calculated contents of helical multipole expected for this helical dipole together with the 2-dimensional multipole coefficients of the 2-dimensional structure for the reference radius r_0 = 30 mm, are shown in Tables 5 and 6, respectively. The twist (or k) dependence of the reference field $B_{ref}(k)$, the helical skew quadrupole coefficient, $a_2(k)$, and the helical normal sextupole coefficient, $b_3(k)$, are also shown in Figs.11, 12 and 13, respectively.

4. Conclusion

The contents of multipole expected for a prototype of the direct wind helical dipole are obtained analytically, with the comparison between helical multipoles and 2-dimensional multipoles. The analytical results are almost consistent with those obtained with the Biot and Savart's Law. It seems that the contents of multipole expected for this prototype of the direct wind helical dipole are much larger than those of the slotted helical dipole. This should be investigated experimentally with the field measurement.

5. Acknowledgments

Special thanks go to AML, Inc. and BNL for providing us with a wealth of information on the RHIC helical dipole magnets. The author is also indebted for helpful discussions and comments to Prof. T. Katayama of Institute of Nuclear Physics, University of Tokyo and RIKEN and Dr. M. Okamura of BNL/RIKEN.

References

1) M. Okamura, "Multipole Components in the BNL Type Helical Dipole Magnet", AGS/RHIC/SN No.46. November 12, (1996).

2) T. Tominaka, "Analytical Field Calculation of the Slotted Helical Dipole", AGS/RHIC/SN No.47, November 12, (1996).

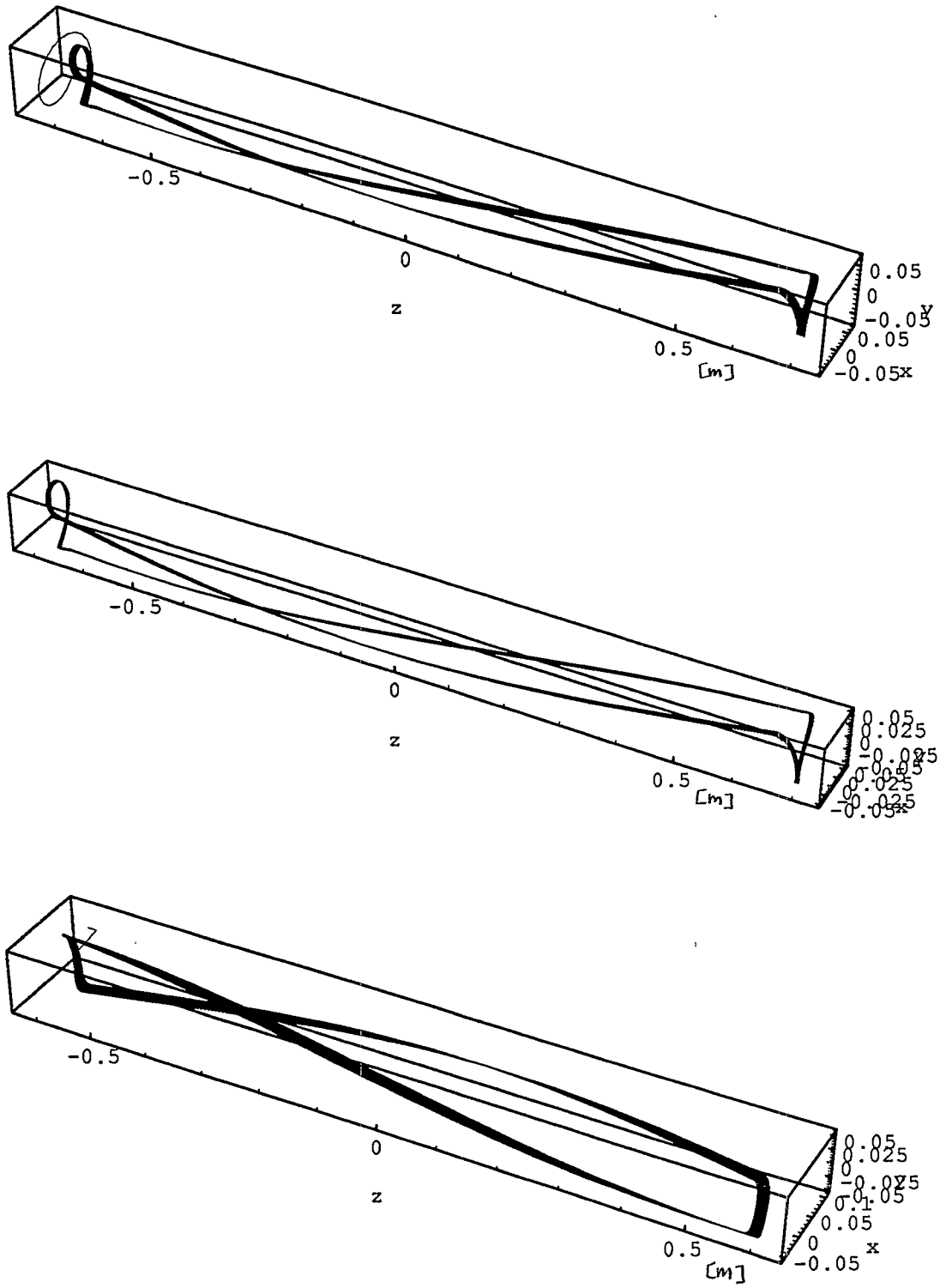

Fig.1 Schematic view of a direct wind helical dipole fabricated in AML, Inc.

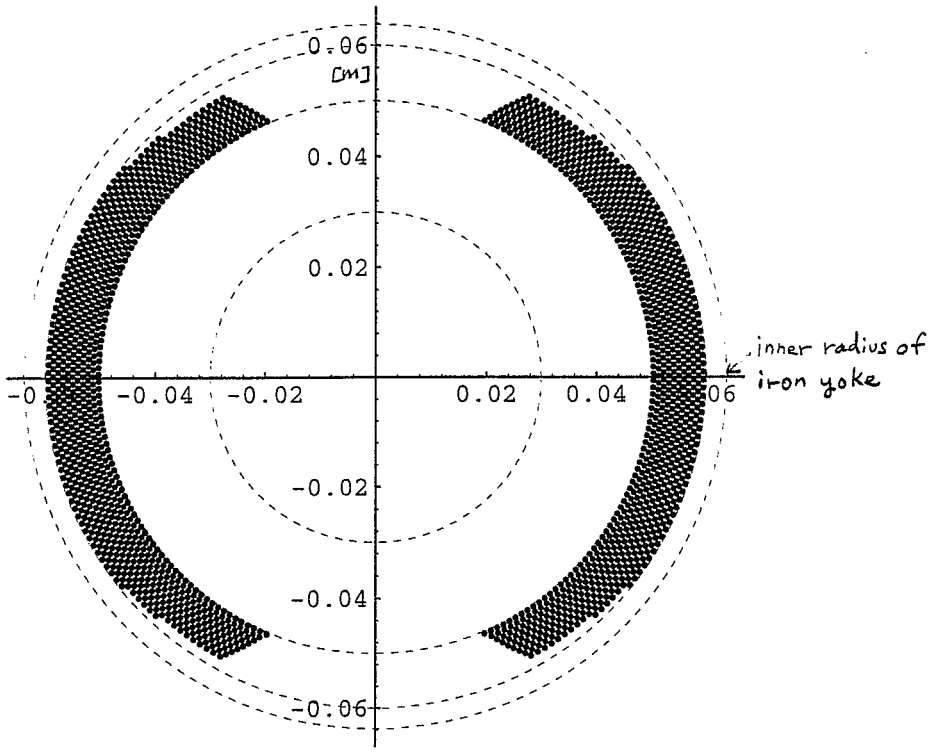

Fig.2 Cross section of a direct wind helical dipole at z=0.

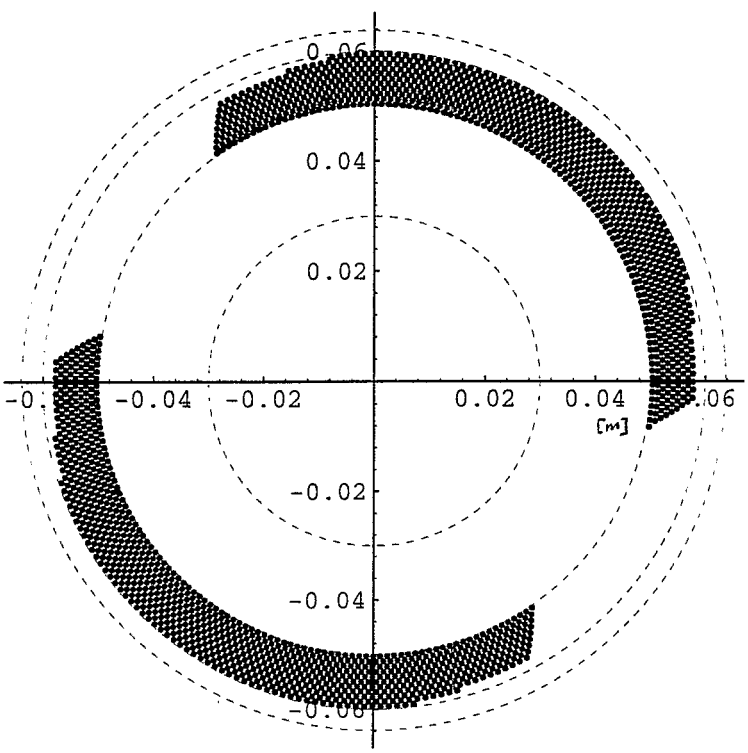

Fig.3 Cross section of a direct wind helical dipole at z=0.4 m.

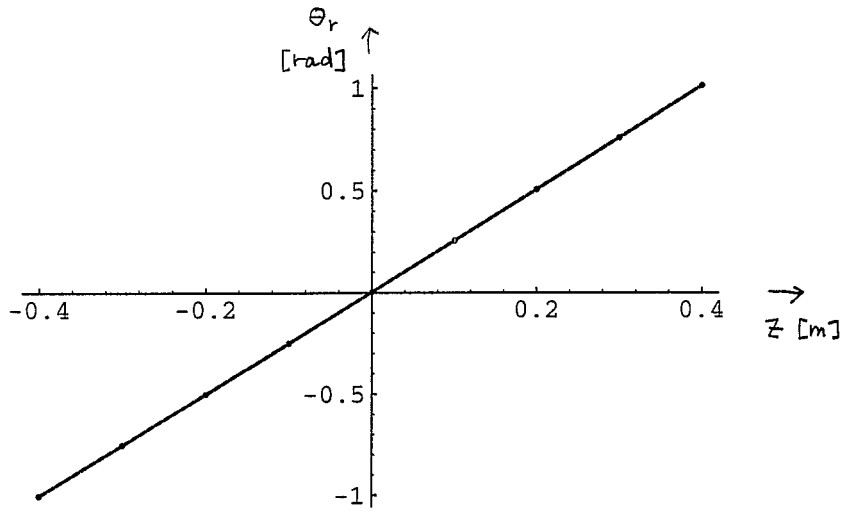

Fig.4 Rotation of the center angle of the right coil block of the helical dipole along the z-axis.

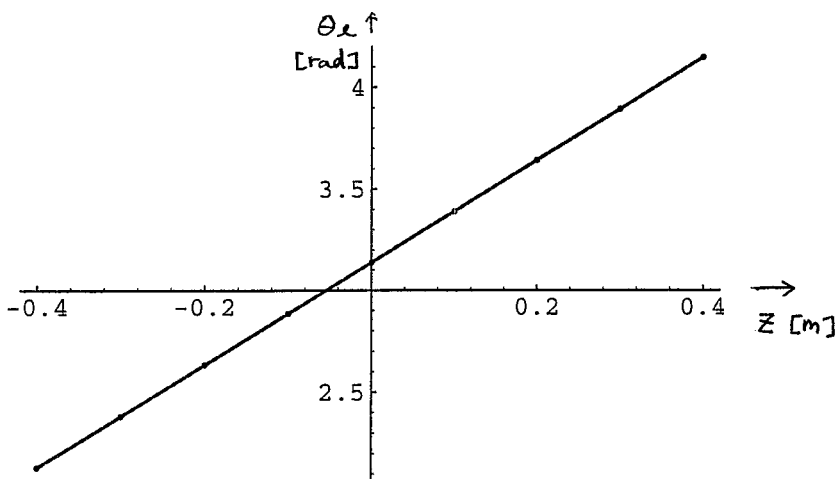

Fig.5 Rotation of the center angle of the right coil block of the helical dipole along the z-axis.

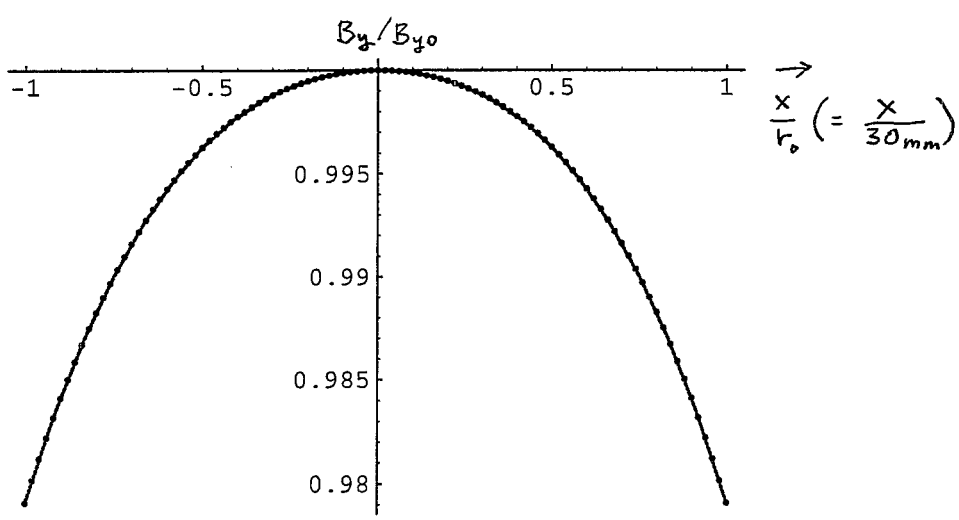

Fig.6 The field distribution of By/By0 on the x axis at z=0.

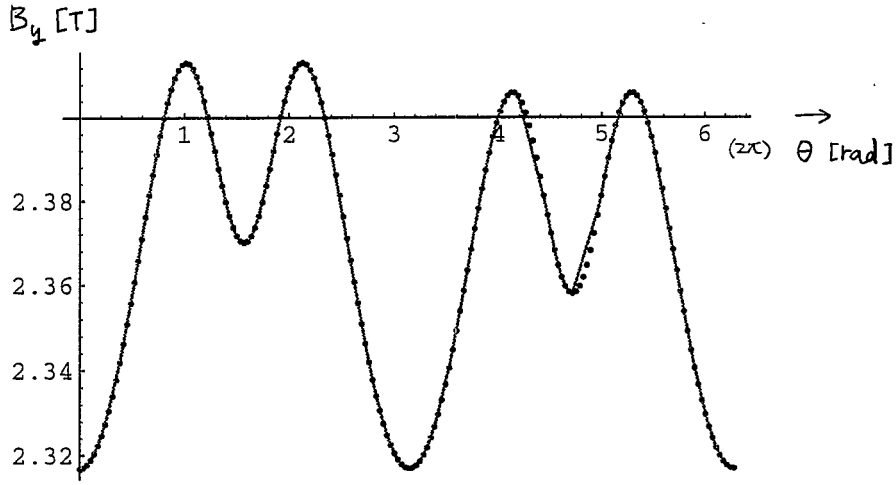

Fig.7 The field distribution of By on the circle of r=30 mm at z=0

Table 1 2-dimentional normal and skew multipole coefficients of By derived with the reference radius r0=30 mm without iron yoke.

n (Bref)	bn-(By) 2.36956 [T]	an-(By)
1.	1.	0
2.	$-1.75642\ 10^{-7}$	0.00195705
3.	-0.0135951	$-2.35355\ 10^{-11}$
4.	$-6.09624\ 10^{-10}$	-0.000557199
5.	-0.0116785	$5.60223\ 10^{-10}$
6.	$-1.41894\ 10^{-10}$	0.0000588584
7.	0.00361183	$-6.71077\ 10^{-10}$
8.	$2.0873\ 10^{-10}$	0.000018266
9.	-0.000669186	$6.27024\ 10^{-10}$
10.	$6.01086\ 10^{-11}$	-0.0000136172

Table 2 Helical normal and skew multipole coefficients derived with the reference radius r0=30 mm without iron yoke.

n (Bref)	bn-r 2.36616 [T]	bn-theta 2.36616 [T]	bn-z 2.36616 [T]
1	0.999858	0.999851	1.00431
2	$2.48807\ 10^{-8}$	$2.48771\ 10^{-8}$	$-7.74459\ 10^{-9}$
3	-0.0128321	-0.0128322	-0.0128167
4	$-4.41862\ 10^{-10}$	$-7.20581\ 10^{-10}$	$-4.44543\ 10^{-10}$
5	-0.0116098	-0.0116098	-0.0116076
6	$4.03327\ 10^{-11}$	$-4.59763\ 10^{-11}$	$2.04921\ 10^{-9}$
7	0.00356022	0.00356028	0.00355938
8	$5.26232\ 10^{-10}$	$-2.88737\ 10^{-11}$	$1.1025\ 10^{-9}$
9	-0.00065549	-0.000655498	-0.000655582
10	$8.03443\ 10^{-10}$	$-1.35233\ 10^{-10}$	$1.06214\ 10^{-9}$

n (Bref)	an-r 2.36616 [T]	an-theta 2.36616 [T]	an-z 2.36616 [T]
1	$4.49751\ 10^{-7}$	$4.4975\ 10^{-7}$	$1.64343\ 10^{-6}$
2	0.00187142	0.00187318	0.00142681
3	$2.45863\ 10^{-10}$	$3.47195\ 10^{-10}$	$2.21019\ 10^{-9}$
4	-0.000553354	-0.00055332	-0.000557709
5	$3.40422\ 10^{-10}$	$6.72358\ 10^{-10}$	$-7.44653\ 10^{-9}$
6	0.0000577292	0.0000576659	0.0000673368
7	$-1.28486\ 10^{-9}$	$-3.70654\ 10^{-10}$	$4.16185\ 10^{-9}$
8	0.0000181349	0.000018154	0.0000155491
9	$3.25262\ 10^{-10}$	$1.683\ 10^{-12}$	$-1.18241\ 10^{-8}$
10	-0.0000133903	-0.0000133916	-0.0000129289

Table 3 Helical normal and skew multipole coefficients derived with the reference radius r0=30 mm for the cross section shown in Fig.1 without iron yoke.

n (Bref)	b-helix 2.37017 [T]	a-helix
1	1.	$-5.58988\ 10^{-17}$
2	$1.07864\ 10^{-16}$	0.00185155
3	-0.0127933	$-1.20763\ 10^{-17}$
4	$-8.18812\ 10^{-18}$	-0.000553554
5	-0.0116381	$1.64106\ 10^{-17}$
6	$6.14109\ 10^{-18}$	0.0000596577
7	0.00358019	$-4.00258\ 10^{-18}$
8	$3.80245\ 10^{-19}$	0.0000175506
9	-0.000662177	$1.34944\ 10^{-18}$
10	$1.00064\ 10^{-19}$	-0.0000134136

Table 4 2-dimensional normal and skew multipole coefficients derived with the reference radius r0=30 mm without iron yoke.

n (Bref)	b-2d 2.33431 [T]	a-2d
1	1.	$2.93541\ 10^{-17}$
2	$1.33765\ 10^{-17}$	0.00188125
3	-0.0130581	$-4.89544\ 10^{-17}$
4	$9.05703\ 10^{-18}$	-0.000569119
5	-0.0120307	$3.42541\ 10^{-18}$
6	$3.93632\ 10^{-18}$	0.0000617629
7	0.00373076	$1.84043\ 10^{-18}$
8	$4.6185\ 10^{-18}$	0.0000184283
9	-0.00069556	$1.39049\ 10^{-18}$
10	$-2.98998\ 10^{-19}$	-0.0000141819

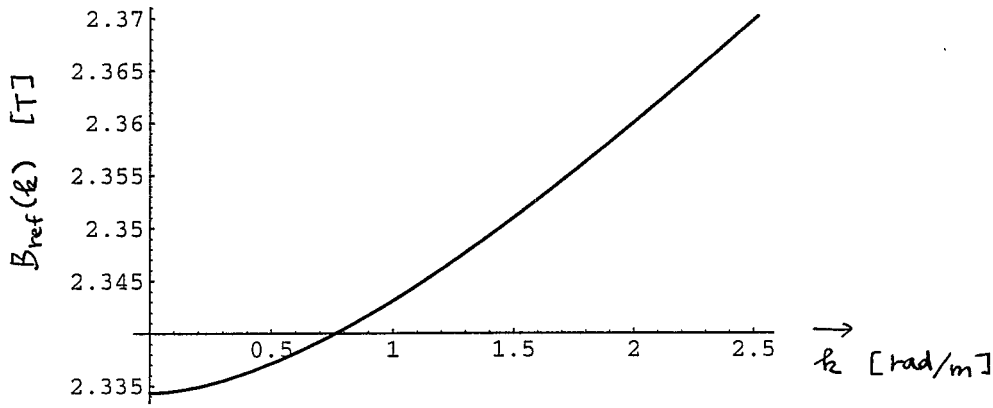

Fig.8 Twist dependence of the reference field Bref(k) without iron yoke.

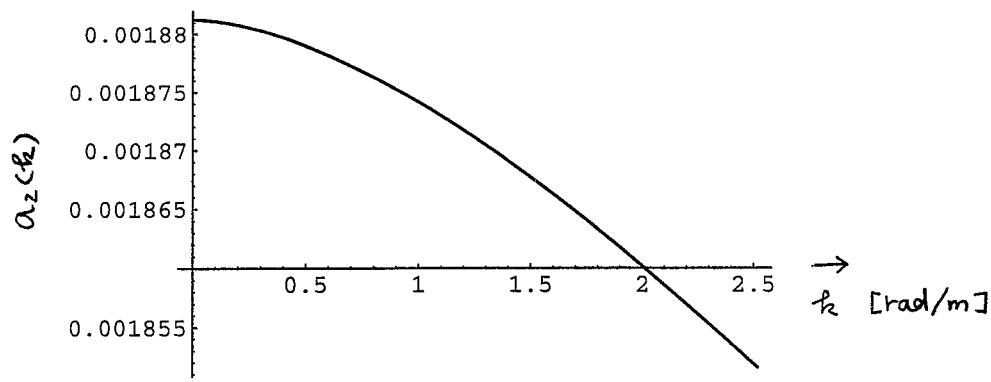

Fig.9 Twist dependence of the skew quadruple coefficient a2(k) without iron yoke.

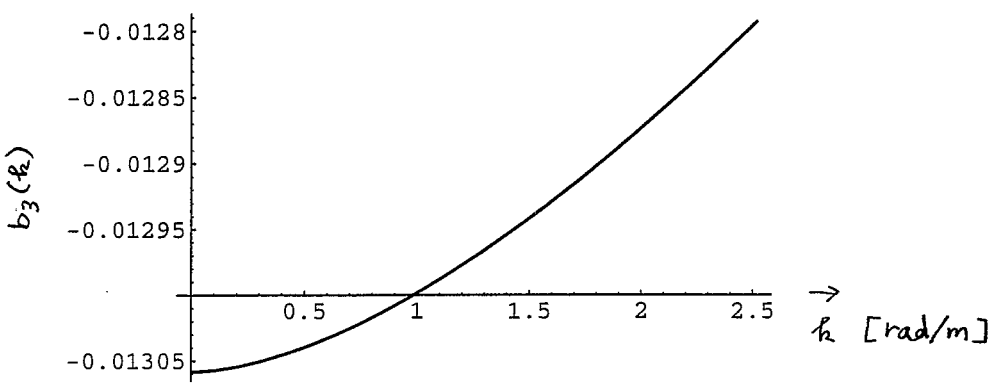

Fig.10 Twist dependence of the normalsextuple coefficient b3(k) without iron yoke.

Table 5 Helical normal and skew multipole coefficients derived with the reference radius r0=30 mm for the cross section shown in Fig.1 with iron yoke.

n (Bref)	b-helix 4.12664 [T]	a-helix
1	1.	$4.8553\ 10^{-17}$
2	$-1.69725\ 10^{-17}$	0.00170723
3	-0.0077653	$-3.83589\ 10^{-18}$
4	$2.85459\ 10^{-17}$	-0.000405037
5	-0.00827777	$4.67664\ 10^{-18}$
6	$3.56659\ 10^{-18}$	0.0000344421
7	0.00221009	$-5.0576\ 10^{-19}$
8	$8.5388\ 10^{-20}$	0.0000111438
9	-0.000389789	$8.83438\ 10^{-19}$
10	$-1.14945\ 10^{-19}$	$-7.92719\ 10^{-6}$

Table 6 2-dimensional normal and skew multipole coefficients derived with the reference radius r0=30 mm for the cross section shown in Fig.1 with iron yoke.

n (Bref)	b-2d 4.05087 [T]	a-2d
1	1.	$-4.76411\ 10^{-17}$
2	$3.62394\ 10^{-17}$	0.00174092
3	-0.00796824	$-3.5597\ 10^{-18}$
4	$5.80794\ 10^{-18}$	-0.000418824
5	-0.00860812	$9.44124\ 10^{-18}$
6	$-7.2733\ 10^{-18}$	0.0000358227
7	0.00231524	$-3.00434\ 10^{-18}$
8	$6.37334\ 10^{-19}$	0.0000117679
9	-0.000411232	$8.30542\ 10^{-19}$
10	$8.36396\ 10^{-21}$	$-8.41906\ 10^{-6}$

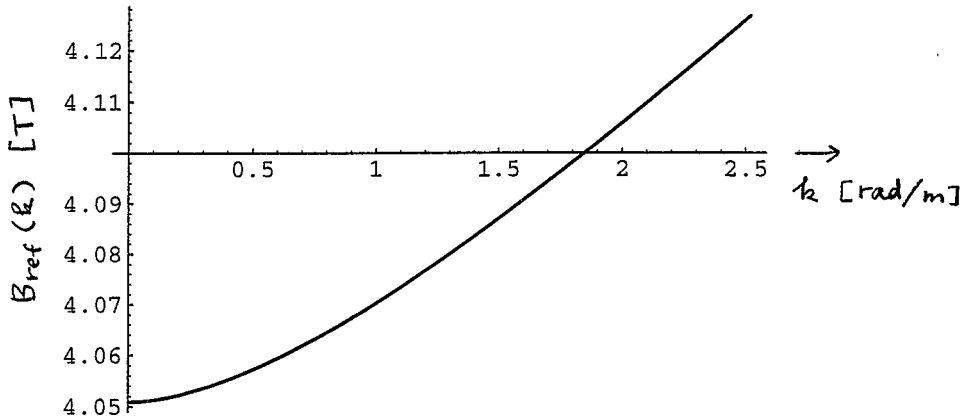

Fig.11 Twist dependence of the reference field Bref(k) with iron yoke.

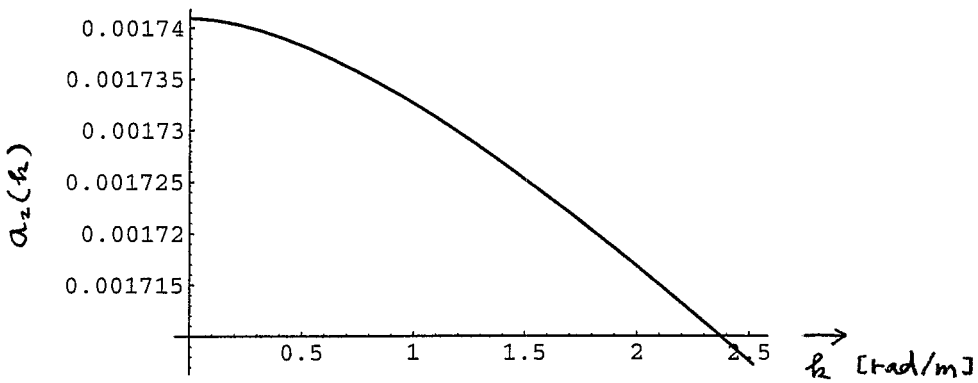

Fig.12 Twist dependence of the skew quadruple coefficient a2(k) with iron yoke.

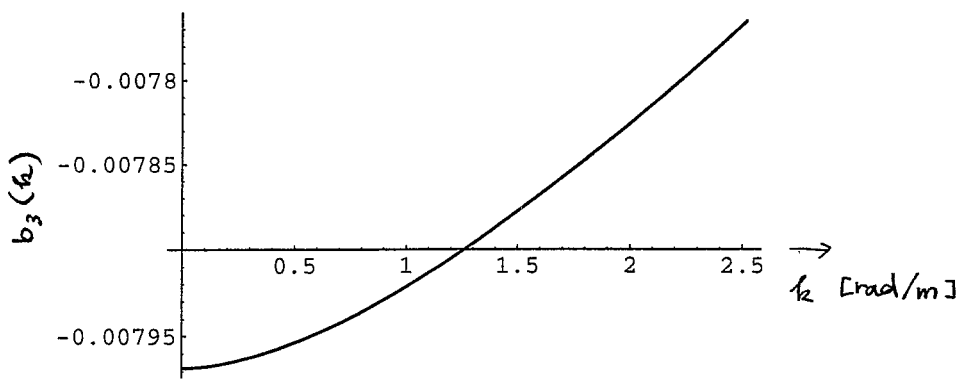

Fig.13 Twist dependence of the normalsextuple coefficient b3(k) with iron yoke.